



HAL
open science

Mechanical Fatigue Testing Under Thermal Gradient and Manufacturing Variabilities in Nickel-Based Superalloy Parts with Air-Cooling Holes

A. Aublet, M. Rambaudon, F. N'guyen, David Ryckelynck, C. Remacha, R. Cariou, Henry Proudhon

► **To cite this version:**

A. Aublet, M. Rambaudon, F. N'guyen, David Ryckelynck, C. Remacha, et al.. Mechanical Fatigue Testing Under Thermal Gradient and Manufacturing Variabilities in Nickel-Based Superalloy Parts with Air-Cooling Holes. *Experimental Mechanics*, 2022, 10.1007/s11340-022-00868-0 . hal-03689137

HAL Id: hal-03689137

<https://hal.science/hal-03689137>

Submitted on 14 Oct 2022

HAL is a multi-disciplinary open access archive for the deposit and dissemination of scientific research documents, whether they are published or not. The documents may come from teaching and research institutions in France or abroad, or from public or private research centers.

L'archive ouverte pluridisciplinaire **HAL**, est destinée au dépôt et à la diffusion de documents scientifiques de niveau recherche, publiés ou non, émanant des établissements d'enseignement et de recherche français ou étrangers, des laboratoires publics ou privés.

Mechanical Fatigue testing under thermal gradient and manufacturing variabilities in Nickel-based Superalloy parts with air-cooling holes.

A. Aublet^{1,2*}, M. Rambaudon¹, F. N'Guyen¹, D. Ryckelynck¹, C. Remacha², R. Cariou² and H. Proudhon^{1*}

¹Centre des Matériaux, Mines ParisTech, 63-65 Rue Henry Auguste Desbrùères, Evry, 91000, France.

²Safran tech, Rue des Jeunes bois, Châteaufort, 78117, France.

*Corresponding author(s). E-mail(s):

axel.aublet@minesparis.psl.eu;

henry.proudhon@minesparis.psl.eu;

Abstract

Background: As aerospace cast parts move to more complex geometries, the impact of process variabilities must be evaluated more precisely to provide new, less empirical acceptance criteria. However, experimental lifetime assessment with Thermal Gradient Mechanical Fatigue (TGMF) are still complicated to reproduce in a laboratory environment. Objective : This paper investigates the impact of geometrical variability on thermo-mechanical fatigue life of Nickel-based superalloy single crystal parts. Methods : To this end, hollow specimens with cooling holes drilled in their centre have been produced with parametrized variations of the wall thickness and have been characterized by X-ray tomography. An experimental fatigue setup operating at 1100°C, with a thermal gradient of 50°C across the wall, has been developed to assess the life of each specimen. Results : Experimental lifetime assessment were conducted on a sample of specimens containing geometrical defects. Optical observations during the tests have permitted to study crack initiation and propagation in the vicinity of the cooling hole, an area of high thermal and stress gradients where damage localize. Axial strains (in the loading direction) were also gathered and

compared to prove the impact of process variabilities on mechanical behaviour. Conclusions : Significant mechanical differences are observed during the tests which can related to the geometrical variations of the specimens and their interaction with the shaped hole. Tests results will be further used to calibrate a creep-fatigue model for lifetime predictions.

Keywords: Thermal Gradient Mechanical Fatigue (TGMF), Lifetime assessment, Single crystal Nickel-based superalloy, Cooling Hole

1 Introduction

Since its inception, the aerospace industry seeks to develop new engines with improved efficiency which depends primarily on the quality of the fuel combustion and the temperature of the gas mixture burned. Increasing this temperature would reduce propellant consumption and the emission of particles harmful to the environment. However, this implies a revision of the engine components' architecture, such as the High Pressure Turbine Blades (HPTB). These innovations are being developed along several lines of research, such as the design of more sophisticated geometries (more efficient cooling systems notably) and the use of new materials. Among them, strong candidates materials are studied as several generation Nickel-based SX [1, 2], other kind of superalloy as Cobalt-based [3] or polycrystalline superalloy [4] and also ceramic composites [5]. Nickel-based superalloys, are well-known in aeronautical industry since a few decades for their mechanical superiority under Creep-Fatigue high temperature loadings as encountered in High Pressure Turbines. To improve combustion efficiency, the turbine inlet temperature have to increase as much as possible, up to record values as mentioned recently in [6]. Such a deleterious environment combine to the cooling system brings the new issue of the lifetime of materials under thermal gradient. On service HPTB are submitted to Low Cycle Fatigue (LCF), Thermal Fatigue (TF) and their combination with creep generate a Thermal-Mechanical Fatigue (TMF) loading. Furthermore, cooling systems also generate a different type of loading called Thermal Gradient Mechanical Fatigue (TGMF) [7]. Those latter have been studied since a few decades through standardization [8] and testings [4, 9, 10].

The main purpose of this work is to characterize a scatter in lifetime due to manufacturing process variabilities, during representative TGMF testing. In this paper, we study a certain kind of damage around a cooling hole drilled on HPTB called Shaped Holes which are morphologically different depending their position. We consider the shaped of holes localized in the top of air-blades where cooling is the most efficient. To generate representative damage, a specific loading case is applied on specimens. It looks like loadings often encountered with Thermal Fatigue where specimens aren't free to deform as seen in the MAATRE test rig [11, 12]. Many works in the literature can be found concerning such kind of testings as the selection of new materials for

aeronautical applications [13] or the study of real HPTB geometries [14, 15]. More precisely on the damaging around cooling holes as the effect of trepanning speed laser drilling [16], through the skew angle [17] and mechanical response [18, 19]. Those experimental roll-out are recently regaining interest since the recent willing of breakthrough in aeronautical developments. While some works have been conducted on standard specimens [19], airblade wise specimen [20] or full-scale turbine-blades [14, 21], very few studies have investigated the local damaging on critical area such as Shaped Holes. Shaped Holes are specific drills machined on the intrados' surface of HPTB and join internal cooling cavities to the external environment. These holes not only allow cooling airflow to escape but also ensure a film cooling effect due to aerodynamic morphology of the drill. A progressive footprint from the intern surface to the external avoid flow aerodynamic stalling and also creates a shell cooling of the blade. However, although the cooling effect allows to improve inlet temperature, it creates a weak point from the structural point of view. Many works have also treated the subject of geometrical accident in structures and their effect on mechanical response under tensile [17], cyclic [18] and LCF loadings [16]. But, so far, no papers concerning damaging generated by TMGF on such complex areas have been found in the literature. Thus, this paper propose an experimental roll-out for lifetime assessment of Shaped Holes under TGMF loading conditions.

The complicated manufacturing process of single crystal superalloy HPTB with internal cavities generate important geometrical variations (local thickness scattering, rotation of the cavity etc.) associated with crystal misorientation which can have a deleterious impact on the structure response. To study this effect, batches of specimen containing such defects have been produced and were tested under TGMF to assess their lifetime. The lifetime considered here is defined by the initiation of cracks of a certain size in the vicinity of the Shaped Hole which is a critical area due to fine geometry and local stress concentration. The material, specimen manufacturing and the TGMF testing set-up are presented in section 2. Then, testing results, lifetime and crack observations are shown in section 3. Results and their use to calibrate a thermo-mechanical model are discussed in section 4. Finally, a conclusion summarizes the main findings of this paper.

2 Experimental methods

2.1 Material

The material used here is a 3rd Nickel-based superalloy called the CMSX4 Plus developed by Cannon and Muskegon [22] with the nominal chemical composition presented in the Table 1.

The CMSX4-Plus, as other Nickel-based superalloys, get a dendritic microstructure composed of a ductile austenitic γ -phase Nickel matrix and γ' -phase hardening precipitates with cuboidal morphology. This alloy is known for getting better mechanical performances than its predecessor (CMSX4) already

Elements	Ni	Cr	Mo	Co	W	Re	Al	Ti	Hf	Ta
Wt. Pct.	Bal.	3.5	0.6	10.0	6.0	4.8	5.7	0.85	0.1	8.0

Table 1: CMSX4-Plus composition.

used in aeronautical industry. This improvements notably under high temperature creep conditions are due to refractory elements adding as (Re, Mo, W) [22]. However, its Re rate is lower than other 3rd SX to decrease weight and axial stresses due to rotation inertia but also lower alloying cost, improve coating compatibility and easy its production. The downside being that the creep-rupture properties are impoverished due to lower Re. In addition, more segregation phases from as cast microstructure are created during manufacturing. Higher temperature Heat Treatment (HT) is needed where Solution Treatment (ST) windows are more and more narrowed (near the alloy melting point). The recommended HT is composed of a ST up-to near 1340°C reached with different dwells to avoid overheating which may lead to alloy melting. The material underwent an Argon quench to fix the cuboidal microstructure followed by an R1 ageing is performed to optimize the precipitates size to about 40 nm [23] at about 1100°C for 6 hours and a relaxation annealing at 870°C for about 20 hours. To appreciate lifetime of the SX material itself we consider here no polish treatment nor thermal barrier coating on the specimens after the manufacturing process.

2.2 Manufacturing single crystal specimens

2.2.1 Production of specimens with geometrical variabilities

The specimens have been manufactured within Safran’s foundry (Gennevilliers, France) where aeronautical parts such as High Pressure Turbine Blades are produced for several motors. Single crystals were obtain thanks to the Bridgman process deployed on investment casting operated under vacuum with solidification gradient control [24].

To make hollow specimens showed in Fig. 1, ceramic cores are injected with a high pressure press. The core represent the inner shape of the final part : a wax coat is injected on the ceramic cores and after casting, it will be replaced by metal. To ensure the single crystal characteristic of the superalloy, a grain selector placed on the bottom of the wax cluster creates a competition of germination direction. A specific shape is designed to select the optimal direction which aligns the [001] crystal axis with the loading direction of the specimen.¹. To represent HPTB internal cavities deviation, a specific core box has been designed and developed as presented in Fig. 2. This latter allows to easily produce ceramic internal cores where diameter can change from a piece to another. Available diameters amplitude are inscribed on the Fig.1.

¹In the first parts produced, due to the specimen’s geometry, piping appeared into shoulders which leads to local metal shrinkage and thus, porosities. To avoid those deleterious defects, unwanted in our study, casting weights have been place there to improve local melted metal repartition but needs a new machining step to remove it after solidification.

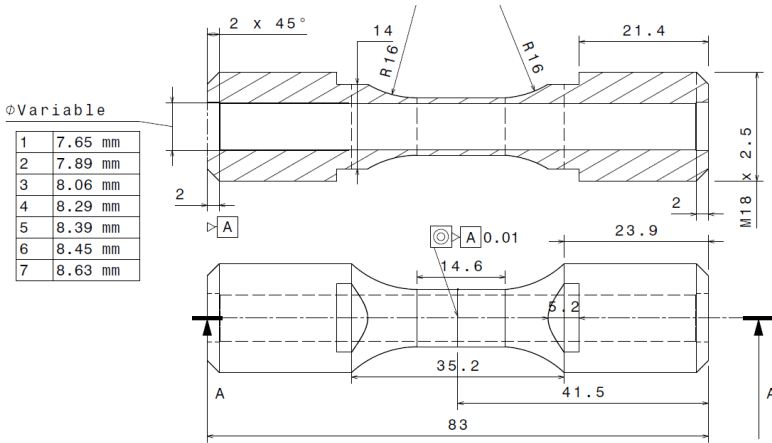


Fig. 1: Specimen drawing : variable internal bore diameter between representative wall thickness (no Shaped Hole drills is represented here for confidentiality reasons).

2.2.2 NDT characterization of geometrical variabilities

To characterize the manufacturing induced geometrical variabilities, several Non Destructive Techniques (NDT) have been applied to the specimens. To appreciate 3D defects and geometrical shape, Computed Tomography (CT) is used. X-Ray (XR) projections (called radiographies) of the part are taken at different angles and reconstruction algorithms are applied to access to 3D volume of the piece where geometrical control can be applied through image processing techniques [25–27]. Although grain selector restrict crystal primary orientation, a misorientation can still occur during casting and have a major impact on mechanical behaviour. NDT are used to measure that disorientation in industry such as, Auleytner X-ray topography [28] or reflection Laue's Diffraction [29]. That technology is based on X-Ray Diffraction of materials coupled to the Bragg's law : a single crystal will have a specific diffraction pattern. The crystallographic disorientation of a given piece may be computed regarding the difference with a reference well-aligned pattern. Used in Safran's industrial process, this technology can provide a misorientation matrix usable in simulation to capture lifetime decrease. The XR acquisition parameters are listed here : for tomography the voltage is about 400 kV, current of 625 A and a power of 450 W, an angular step of 0.14° , a time exposure of 350 s, 2500 radiographies acquired and a final voxel size of 29.45 μ m. The Laue diffraction parameters are different : the voltage is about 50 kV, current of 40 mA and a power of 2 kW and a pixel size of 400 μ m.

All the manufacturing steps can induce variabilities (geometrical, metallurgical, crystallographic) on the parts which can interfere with on-service mechanical behaviour. Furthermore, newest and future high pressure turbines air foils will propose more complex geometries linked to motors' efficiency

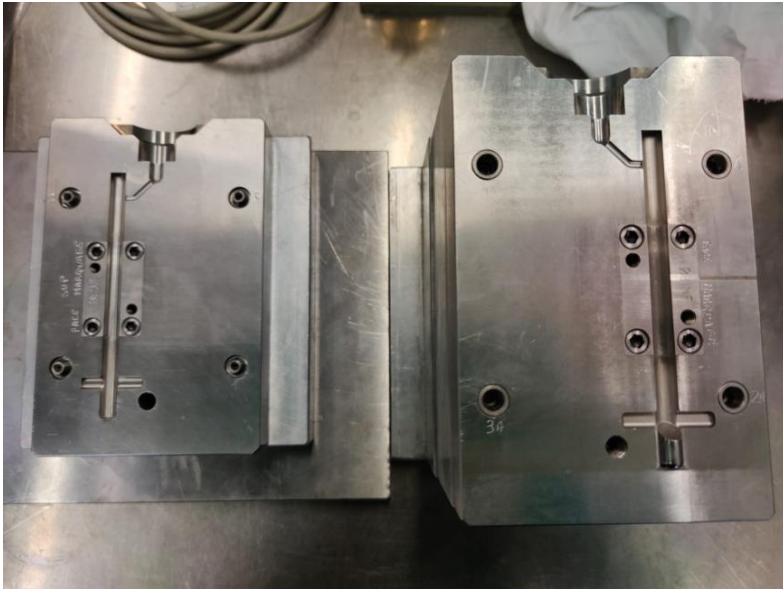


Fig. 2: Core box : adaptable component for wax injection.

improvements. Current methods employed in aeronautical industries control a huge quantities of local indicators (as geometrical hot spots), without taking in account the local vicinity. The reason is the difficulty in parametrizing such geometrical scattering on CAD models due to 3D curved shapes like HPTB. We are taking a new approach to digital twin strategies to ease manufacturing control and analysis [30, 31]. The last part of the manufacturing process is the Shaped Hole drilling. Those drills are machined using Electrical Discharge Machining (EDM) methods where metal is removed by high frequency electrical discharges using a brass electrode. The machining is made one layer at a time and allows to create complex hole shapes as those consider in this work. A SEM picture of a Shaped Hole is visible later in the manuscript, in Fig. 12. Representative geometry can be found in [32] where several geometries of cooling holes are listed. From a mechanical point of view, such geometries generate a stress concentration factor of approximately 3.5.

The geometrical variabilities can be either global as eccentricity of the inner cylindrical bore or local as roughness (not considered in the study). The global geometrical defects can change the section uniformity and consequently, the load repartition in the structure. In particular, local stresses around the hole can be affected by the process repeatability and strongly impact the structure response.

2.3 Thermal-mechanical loading

The mechanical loading consist in the repetition of simplified flight-like solicitation inducing specific stress states. The cycle is composed of a take-off

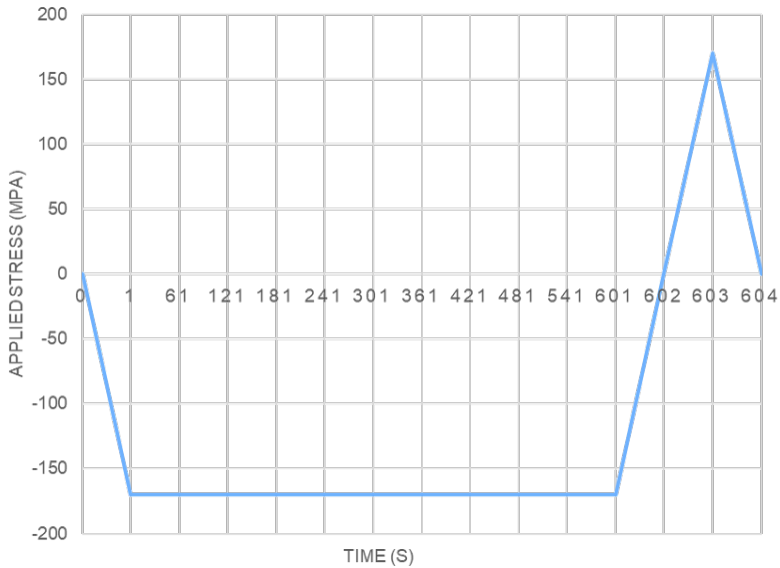


Fig. 3: Definition of the loading cycle : 1 cycle lasts about 10 minutes and is repeated 120 times.

(compressive state) followed by the landing stage which, due to plastic strain appearing during compression, generates a tensile state. The cycle is presented in Fig. 3. The 10-minutes long cycle has been chosen to recreate the thermal cooling effect of future blade geometries where compression due to thermal cooling may overpass the tensile state generates by inertia with engine rotation. The stress in the gage zone is set to 170 MPa which is slightly higher than the stress value near this kind of area on airblades. The target force required to impose the stress state is computed precisely thanks to the CT measurement of each specimen (see Section 2.2.2). This cycle lasts about 10 minutes long and is repeated 120 times to create a 20 hours uninterrupted testing, resulting in a creep-fatigue coupled damage occurring around the drill which represents 120 take off - landings (the cruise stage is neglected here). As we consider tubular specimens under compressive loading, buckling risks have been investigated with FEA simulations and checked with a sacrificial part.

A thermal loading is also applied with a heating at 1100°C which approximates the service temperature seen by the material under the thermal barrier usually applied on airblades. Finally, to perform TGMF experiments, fresh air extracted from the laboratory air network is injected inside the specimen with a 7 bar pressure. This way, air cooling is performed on the inner surface of the specimen and airflow escapes by the hole, as presented on Fig. 4.a). The inhomogeneous heating and the wall thermal gradient generated by the fresh air induce an heterogeneous thermal dilatation field and thus a stress state in the Shaped Hole.

2.4 Experimental set-up

The set-up is composed around an electro-mechanical tensile INSTRON 4505 test machine. It allows to perform tensile-compression Low Cycle Fatigue with a frequency up to a few Hz. Considering the cycle presented on 3, the PID controller of the machine is sufficient to apply the loading direction inversion within a second. The load applied to the specimen is measured by a 10 kN load cell. To avoid parasitic torsion or bending effects, a high degree alignment is carried out with a reference piece. The grips are set in a pot containing Wood metal which, once melted, permits free rotation for alignment. The specimen is blocked by threaded grips on each side of the tensile machine with locknuts to prevent the possible release caused by creep. The specimen is heated by a 6 kW radiation furnace composed of 4 infrared (IR) bulbs placed in ellipsoidal prints to maximize the heating flux in the furnace's central axis. The internal surface of the furnace is mirror-polished to improve the reflection of radiative flux to the specimen. The furnace can be seen opened and through a CAD on Fig. 4b). This kind of furnace uses the radiative behaviour of metals for surface heating of samples. Here, considering Nickel-based SX, the test temperature can be reached using only a little more than half of the maximal power in a few minutes. To provide a wall thermal gradient along the specimen, fresh air is extracted from the laboratory pressurised air grid. A debit controller allows to control the airflow debit arriving in the system with flexible pipes. Air arrives in the test machine by the fixtures drilled to help cooling under high temperature testing. Several copper joints are placed between the fixtures and machine bars to ensure tightness and force the airflow to cross the specimen. All critical parts of the machine test as mechanical jaws, fixtures and heating furnace are cooled with pressurized cold water. The water is brought to the different systems with the black and yellow flexible wires visible on the right side of Fig. 5. To limit the axial thermal gradient and create the cooling in the Shaped Holes, air is injected from both sides of the specimen and escapes in the furnace. The strain measurement is made with a ceramic extensometer placed over gauge zone with a length of about 10 mm and provides strain measurements up to $\pm 5\%$. Due to the low range of measurements and as the thermal loading is almost constant, we can reset the extensometer to only measure the mechanical (elastic and inelastic) deformation.

Acquisition system

During the experiment, data from several sources is gathered with different acquisition systems. The main controller is a Labview program developed to perform TMF tests. As the loading is stress-controlled, the program compare the actual state of loading using the load cell and adjust instructions on the PID controller each 100 ms. Additional data are gathered as extensometer strain measure, displacement applied by the tensile machine and acquired by a National Instrument BNC-2110 connexion block. Thermosensors temperature are stored in another acquisition central Hioki LR8431-20 connected by

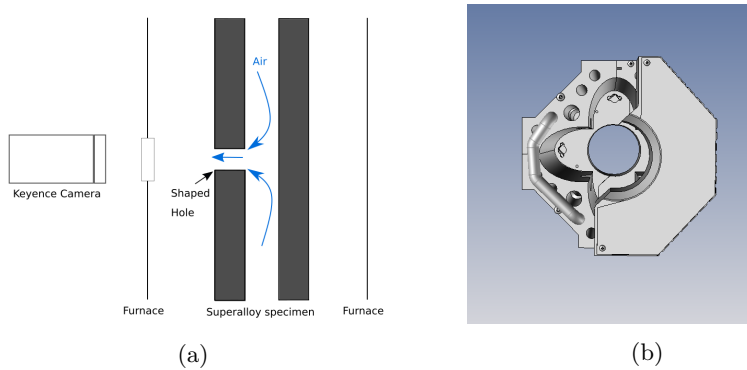


Fig. 4: (a) Definition of the loading cycle : 1 cycle lasts about 10 minutes and is repeated 120 times and (b) CAD model of the furnace with two ellipsoidal bulb footprints.

coaxial wires. To observe crack initiation on the external surface, a high definition microscopy Keyence camera is used. To limit the amount of pictures taken during the 20 h-long experiment, the camera acquisition frequency is synchronised with the current loading state : pictures are taken within 1 Hz during the tensile, compressive and unload phase while 1 picture per minute is acquired during the compressive dwell. An example of the Keyence camera and its position in front of the machine testing is proposed on Fig. 5. As shown, the use of an optical microscopic implies a short working distance (distance between the camera and the object) and in our case it has to be very close to the furnace's wall. A Pyrex glass cup is placed in front of the camera to prevent any damage by the hot air gases escaping. The use of this kind of camera is justified by the fact that the hot gases plume disturbs the internal optical index which provokes important noise on pictures. A typical pre-deformation image is presented on Fig. 12 where a Shaped Hole is centred in the picture with 3 thermosensors welded around it. The measures of the three sensors T1, T2 and T3 are presented in the Fig. 7 and T_{reg} is the regulation thermocouple.

3 Results

3.1 Thermal measures

Heating systems for mechanical testings of metals usually fall into two main categories : induction heating [14, 33, 34], and infrared heating [9, 35, 36]. The former category allows to heat complex parts where thermal fields are hard to generate and can be regulated with a pyrometer. However, copper spires circle the specimen and hide an important part of the geometry during testings which can interfere with optical camera acquisitions. In the present case, an IR furnace has been used. Although well adapted for metals, the radiative heating

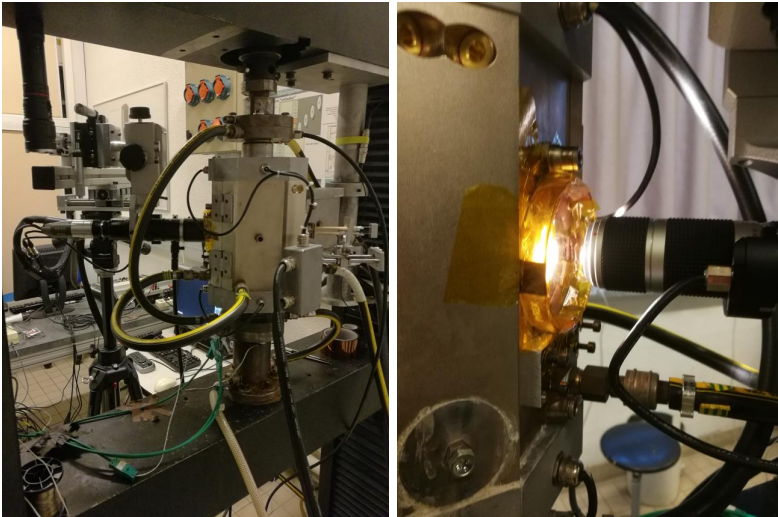


Fig. 5: Keyence camera position in front of furnace (left) and image from behind (right) of the furnace where we can see the ceramic extensometer.

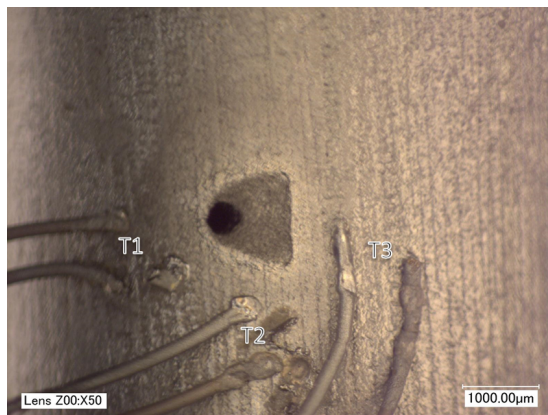


Fig. 6: Shaped Hole at 1100°C in the furnace: presence of 3 thermosensors for temperature acquisition.

efficiency is strongly dependent of several parameters such as the geometry's shape, the metal thickness, the presence of asymmetry or the camera-object distance. The furnace considered in this work is monitored by a PID-controller and a thermosensor welded at the back of the specimen. However, the thermal calibration is delicate due to incompatibility with IR camera and high spectral reflectance materials as Nickel-based superalloy. The main reason is that IR lamps emit radiative heating which is absorbed, reflected and transmitted by the specimen. While an IR camera catches the emitted radiation of a heated

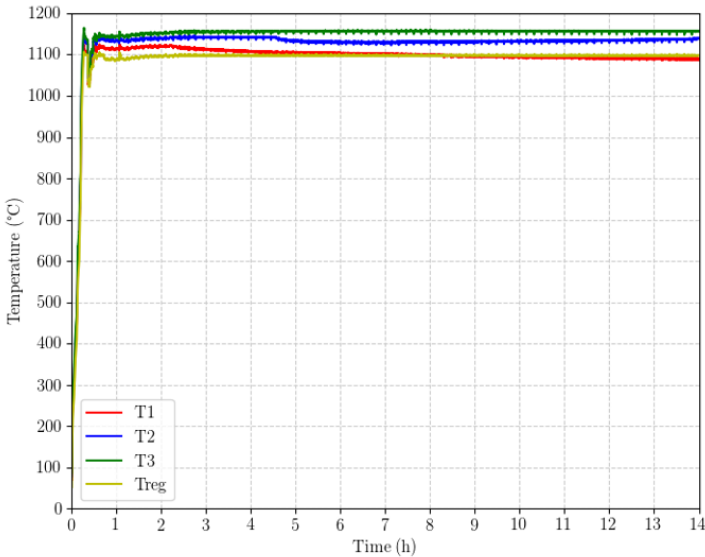


Fig. 7: Surface temperatures around the hole.

solid, the reflected part of the lighting is also measured and strongly affects the acquisition. To control the heating, a calibration campaign was realized with several unshielded K-type thermocouples welded in different parts of the specimen during calibration testings. The curves presented on Fig. 7 demonstrate that even if it's a non-uniform field due to heating anisotropy and cooling gradient, it can be considered as constant over time after a few hours. This delay is due to warmed air contained inside the furnace which affects heating efficiency. One of the main difficulty was the measure of the thermal gradient generated by fresh air. As the inner diameter is too small to weld thermosensors inside, a blind drill using EDM process with a 0.4 mm diameter was done. A thermocouple was inserted inside to measure the wall temperature and glued with a ceramic paste in the specimen half-way up. Subtracting the surface thermocouple measure, we obtain the temperature difference responsible of the radial temperature gradient. The results are presented on Fig. 8 and we can observe that the wall gradient is about -50°C (in the radial direction, through the specimen width) over the $700\ \mu\text{m}$ thickness of the wall, corresponding to the desired cooling value for this work. Once the steady state is reached, within a dozen of minutes, the mechanical loading can be applied.

3.2 Mechanical results

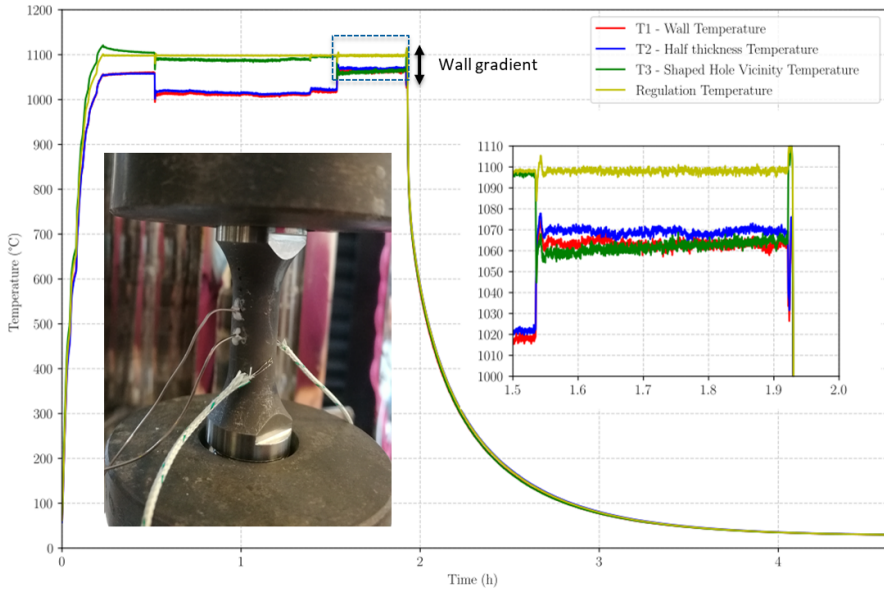


Fig. 8: Wall gradient measures.

The thermal strain ε_{th} can reach 2% for the target temperature and must be removed to access the mechanical strain ε_m , as shown in Fig. 9. We can observe that due to the compressive loading, mechanical strain is negative and increases over time. The tensile part of the loading create a fast positive spike of ε_m which promote cracks initiation and increase damage. The strain non-linearity observed is induced by both viscoplasticity (highly active at such temperature) and creep due to stabilized compression phases. Fig. 10. shows the engineer strain-stress curve during the test carried-out in force-controlled mode and where strain is free to accommodate. A strong ratcheting effect is observed, which prevents strain-stress loop stabilization overtime. It's a well known phenomenon observed with high temperature non symmetric loading magnified by the fact that the yield stress decrease strongly with temperature [37–39]. Ratcheting is a gradual increase of plastic strain, with viscoplastic strain and creep contributions, and blocks strain stabilization. Mechanical strain reaches important values at the end of the experiment for about -3% on the gage zone. The local strain in the hole are even more important, knowing that stress concentration factors that can reach to 3 or 4, depending on the skew angle [17]. We deduce from mechanical measures that such loading state generates high stress-strain response and causes important plasticity localisation in the hole region. This generates high damage and leads to crack initiation we can observe with the optical set-up deployed.

To quantify the impact of the variability obtained during the fabrication process on lifetime, several specimens containing geometrical defects and materials misorientation were tested using the set-up. The observed scatter

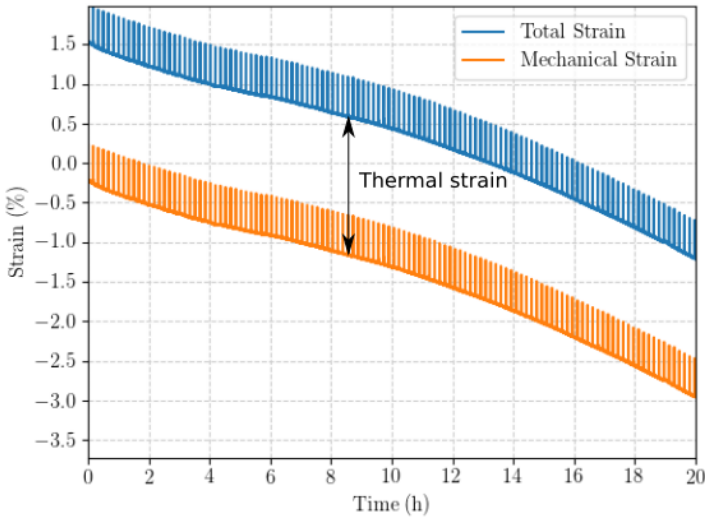


Fig. 9: Total and mechanical strains as a function of time for the complete test of 120 cycles.

of mechanical response for different parts is presented in Fig. 11. The latter shows an important impact on the mechanical strain : parts with identical core diameter form a cluster (formed by specimens 1, 3, 4, 5 and 6) with near strain evolutions between 0 and -0.5 % while specimens 7 and 10 have different responses with a -3% strain gap. This scatter is highly linked with geometrical defects as core movements which modifies the thickness in the section and thus, the stress repartition and crystalline disorientation which drives the material anisotropy. As presumed, the geometrical defects affect the structure response and thus, crack initiation in the hole.

To evaluate lifetime, a crack length criterion is used. Crack propagation is measured on the surface of the specimen with the pictures obtained during the experiment see Fig.6. Thus, the fatigue life is reached once the main crack is 300 μm long. The following table summarizes the lifetime of the 10 specimens presented in Fig.11.

3.3 Optical and SEM observations

As presented before, the lifetime is assessed through cracks initiation on the specimen. The Shaped Hole is a critical area where thermal and stress gradients localize damage. Local plastic strain in the hole cannot be directly accessed but crack initiation and propagation is observed thanks to the Keyence camera (Fig.5) to the external surface. Also, Scanning Electron Microscopy (SEM) imaging was carried out with a Zeiss Sigma microscope before and after testing.

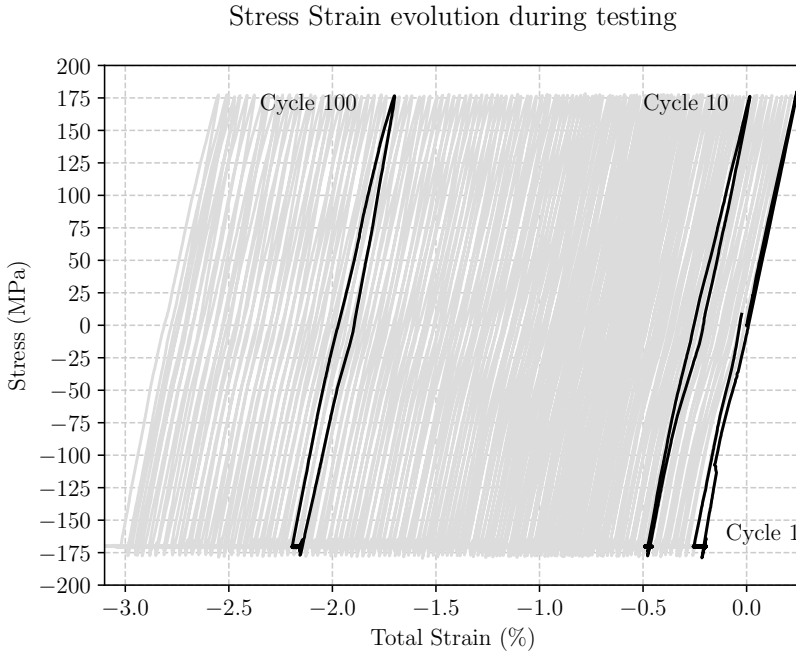


Fig. 10: Cyclic stress-strain evolution with highlighting of the first, tenth and hundredth cycles (b).

Specimen ID	Lifetime (in cycles)
1	61
2	117
3	120
4	61
5	77
6	89
7	78
8	57
9	111
10	92

Table 2: Specimen lifetime in cycles using crack length criterion

Fig. 12 shows the complete drill on the surface before testing. As the Shaped Hole is drill with EDM techniques, the electrode creates a layer-by-layer melting and generates strata perceptible on the picture. The process modifies a local area around the surface called the depletion or recast area, where the alloy is melted with the EDM electrode's brass, as observed in [40]. Then, the Shaped Hole is not only a stress concentrator intensified with the thermal gradient, but also a local area of mechanical weakness. To improve the cooling effect on HPTB as mentioned in section 2.2, the hole is composed of two sides :

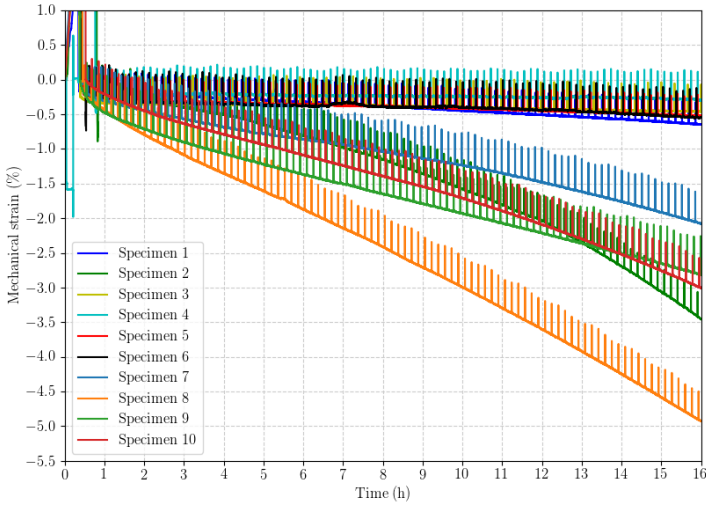


Fig. 11: Experimental strain curves scatter : effects of geometrical variations and crystal misorientation.

one side of constant angle between the two surfaces and the other side with two angles, observable on the SEM picture. To complete our experimental observation, another SEM investigation was realized after the experimental testing, presented on Fig. 13. One may observe that two major cracks initiate in the depth of the drill and propagate toward the external side of the specimen, highlighted by the black arrows. Our study focuses on the initiation phase, which is commonly restricted to maximum crack length of $300 \mu\text{m}$ [41]. Here, the main crack (on the right side of Fig. 13) has a length of about $600 \mu\text{m}$. In that respect, we can consider that the lifetime criterion has been reached. However the post-mortem specimen demonstrates a high corrosion of the drill, due to high temperature and airflow. It is well-known that corrosion creates brittle material phases which depletes the mechanical behaviour of the superalloy [16, 42]. The border of the drill, which is a depletion area, is highly affected by oxidation after testing where local airflow turbulences affects the oxidation, as the differences of corrosion pattern in the hole shows it. In the vicinity of this oxidation effect, stress concentration increases in respect with the impoverishment of mechanical behaviour. The focus on the low-right picture of the Fig. 13 shows that cracks follow a privileged path among the chaotic oxidized microstructure. This path is correlated with plastic strain localization, almost perpendicular with the loading direction.

To go beyond surface oxidation and assess the superalloy damage underneath, a Computed Tomography (CT) scan has been conducted on the post mortem specimen. After reconstruction, the volume rendering and three orthogonal planes slices are presented in Fig. 14. The volume rendering demonstrates that cracks initiates in the acute side of the drill as observed by Zhou

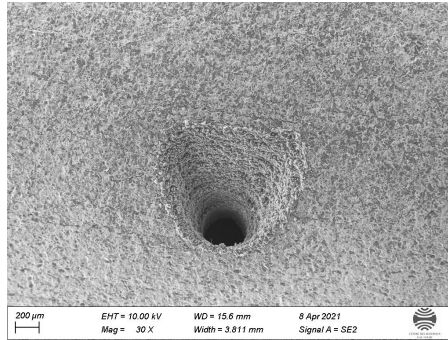


Fig. 12: SEM observed Shaped Holes before testing.

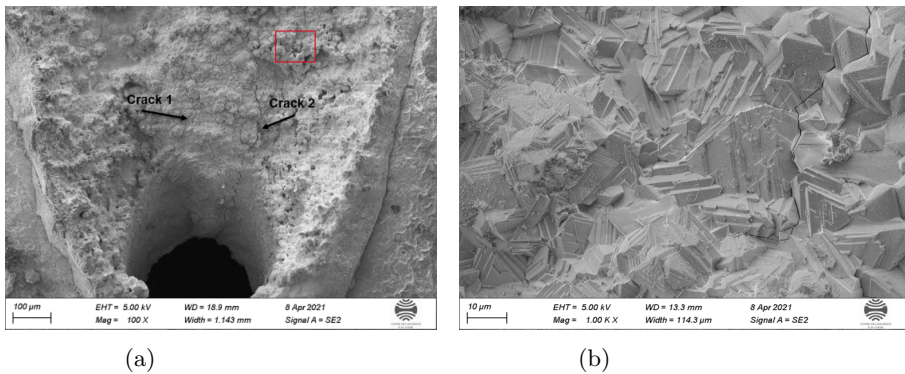


Fig. 13: SEM micrographes of the Shaped Hole after testing : observation of two main cracks (a) and zoom in the hole : focus on the right crack and observation of oxidation (b).

[17]. The ARAMIS system deployed in his work, used to measure strain during testing, showed that stress concentration is highly linked with the skew angle of the Shaped Hole. The lower angle implies the highest local stress state and thus, foster local damage and cracks initiation. The orthogonal slices prove that cracks propagate in the volume and follow the drill morphology until the outer surface.

4 Discussion

The testings presented in this work are supposed to represent simplified damaging loading of HPTB on fatigue specimens. Due to their complex geometries, a simple synthetic HPTB loading is hard to reform in laboratory conditions. The loading shape presented in Fig. 3 propose an unconventional form designed under equivalent creep stage of aircraft's engine mission-like loading. The creep plateau has been reduced and the loading improved to recreate HPTB-like

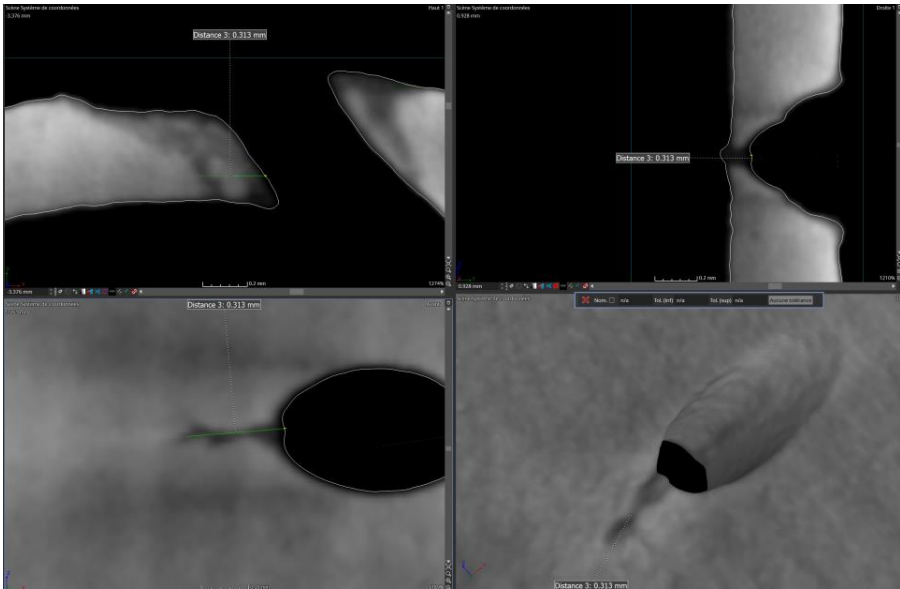


Fig. 14: Post mortem CT scan of specimen and 3D observation showing crack propagation around the shaped hole realized with *VG Studio* software.

damage conditions in short time to ensure a sufficient overview of the behaviour response of the parameters scattering. The tests performed in this work allow to study the impact of compressive creep around cooling holes, which may occur on the future HPTB geometries with new cooling systems. The experiment results representativeness compared to real geometries is practicable due to the dimensional ratios that ensure a scale separation between the local hole and the structure. The sample's geometry originates from High Pressure Turbine Blade geometry to study the lifetime scatter around shaped holes under thermo-mechanical loading. We study the impact of a "crossing section artefact" as a shaped hole which provokes an important stress concentration factor which localizes plasticity. The principle of scale effect is complicated to apply in our case due to the presence of the hole and we do not consider the impact of smaller defects as casting porosity. Also, varying the thermal load applied to the specimen has not been carried out in this work and can presumably have an important impact on the fatigue life results.

During the thermal calibration, field measures were considered using a FLIR IR camera. An IR camera performs thermal measure by computing the radiative balance equation using the material emissivity which strongly depends on the surface's aspect (polished or oxidized), topology (smoothness or drilled area) and the environment (atmosphere, distance, obstacles). Here, the material is not painted nor coated and the lamps reflection is catch in the measures which strongly affects the computed temperatures and remains difficult to extract from field measures. To avoid this issue, calibration tests were

led where thermosensors were welded at different spots from a test to another. This measure allowed to reconstruct a gappy experimental thermal field of the external surface. For each test, a few thermosensors are welded to catch the thermal experimental scatter to calibrate the thermal model for further simulations. Furthermore, the wall thickness measures carried out by a blind hole permit to obtain an estimation of wall gradient to improve the model. Still, no techniques were available to estimate the thermal field around the Shaped Hole, which could be extremely useful for damaging understanding. Thus, the test rig isn't a high fidelity experimental testing still able to manage lifetime assessment for our study.

Finally, lifetime can be deduced regarding the crack propagation in the structure during the test when it appears on the external surface (at least in the area covered by the Keyence camera) or with post-mortem specimens using CT reconstruction. Those measures do not allow a progressive tracking of crack propagation but provide data to calibrate a pseudo propagation rate and 3D cracks lengths computations can be compared to highlight lifetime hierarchy.

Although the acquisition set-up could be enriched to gain accuracy, the strain and thermal measures have permit to calibrate a thermal-mechanical model for FEA simulations and lifetime computations. An existing Meric-Cailletaud [43] behaviour model identified on the CMSX4-Plus will be used and the thermal model will be registered using the several thermal tests realized during the calibration stage. Then, the Fat-Flu damage model will be applied in a post-processing step to assess to lifetime. This model will be the cornerstone for the following work consisting in lifetime prediction using Digital Twin of the mentioned fatigue specimen.

5 Conclusion

The present paper exposes the lifetime assessment of Shaped Hole on Nickel-based Single Crystal superalloy specimen under TGMF conditions ($T = 1100^{\circ}\text{C}$, $\sigma = 170\text{ MPa}$ and $R \approx -1$ with a dwell phase during the compression loading). Noticeable effects of thermal gradient on superalloy damaging have been observed with SEM snapshots and CT scan and led to several conclusions :

- The experimental set-up presented allows assessing simplified still representative in service loading conditions for Shaped Hole damaging under mechanical and gradient thermal loading in a laboratory environment.
- The thermal gradient was characterized to be 50°C in the test conditions.
- Lifetime is deduced by cracks initiation observed in the Shaped Hole which is a critical area due to the fine geometry and local stress concentration.
- At very high temperature levels such as 1100°C , oxidation forms an important part in the damage and generates a brittle phase which locally lower the mechanical resistance of the structure.
- The measured mechanical behaviour evolution during the tests will be further used to calibrate a Creep-Fatigue model for lifetime prediction.

6 Acknowledgement

The authors would like to thank the Association Nationale de la Recherche et de la Technologie (ANRT) for its financial support on this work. We also thank the technical support in the Centre des Matériaux (Atelier JPE and Franck B. notably) for their help in the set-up deployment. We also would like to thank Mr. Ramzy Bohli for his work on the adaptable core box which was the starting point of this work.

Finally, this work is in memory of Alain Köster, as no test would have been possible without his kindness, technical knowledge and passion.

7 Compliance with Ethical Standards

Conflict of interests The authors have no conflict of interest to declare.

References

- [1] Pineau, A., Antolovich, S.D.: High Temperature Fatigue of Nickel-base Superalloys A review with special emphasis on deformation modes and oxidation. *Engineering Failure Analysis*, vol. 16 **16**(8), 2668–2697 (2009) <https://doi.org/10.1016/j.engfailanal.2009.01.010>
- [2] Ormastroni, L.M., Mataveli Suave, L., Cervellon, A., Villechaise, P., Cormier, J.: LCF, HCF and VHCF life sensitivity to solution heat treatment of a third-generation Ni-based single crystal superalloy. *International Journal of Fatigue* **130**, 105–247 (2019). <https://doi.org/10.1016/j.ijfatigue.2019.105247>
- [3] Chung, D.-W., Daniel, S.N., Dunand, D.C.: Influence of γ' -raft orientation on creep resistance of monocrystalline co-based superalloys. *Materialia* **12**, 100–678 (2020). <https://doi.org/10.1016/j.mtla.2020.100678>
- [4] Sun, J., Yuan, H., Vormwald, M.: Thermal Gradient Mechanical Fatigue Assessment of a Nickel-Based Superalloy. *International Journal of Fatigue* **135**, 105–486 (2020). <https://doi.org/10.1016/j.ijfatigue.2020.105486>
- [5] Halbig, M., Jaskowiak, M., Kiser, J., Zhu, D.: Evaluation of Ceramic Matrix Composite Technology for Aircraft Turbine Engine Applications, (2013). <https://doi.org/10.2514/6.2013-539>. <https://arc.aiaa.org/doi/abs/10.2514/6.2013-539>
- [6] Yin, F., Gangoli Rao, A.: Performance analysis of an aero engine with inter-stage turbine burner. *Aeronautical Journal* **121**, 1605–1626 (2017). <https://doi.org/10.1017/aer.2017.93>
- [7] Wang, R., Jing, F., Hu, D.: In-phase thermalmechanical fatigue investigation on hollow single crystal turbine blades. *Chinese Journal of*

- Aeronautics **26**, 1409–1414 (2013). <https://doi.org/10.1016/j.cja.2013.07.026>
- [8] Maurel, V., Köster, A., Rémy, L.: An analysis of Thermal gradient impact in thermalmechanical fatigue testing. *Fatigue & Fracture of Engineering Materials & Structures* **33** (8), 473–489 (2010). <https://doi.org/10.1111/j.1460-2695.2010.01449.x>
- [9] Chaboche, J.L., Jung, O.: Application of a kinematic hardening viscoplasticity model with thresholds to the residual stress relaxation. *International Journal of Plasticity* **13**(10), 785–807 (1997). [https://doi.org/10.1016/S0749-6419\(97\)00066-1](https://doi.org/10.1016/S0749-6419(97)00066-1)
- [10] Hähner, P., Rinaldi, C., Bicego, V., Affeldt, E., Brendel, T., Andersson, H., Beck, T., Klingelhöffer, H., Kühn, H.-J., Köster, A., Loveday, M., Marchionni, M., Rae, C.: Research and development into a European code-of-practice for strain-controlled thermo-mechanical fatigue testing. *International Journal of Fatigue* **30**(2), 372–381 (2008). <https://doi.org/10.1016/j.ijfatigue.2007.01.052>
- [11] Cormier, J., Mauget, F., Le Graverend, J.B., Moriconi, C., Mendez, J.: Issues related to the constitutive modeling of ni-based single crystal superalloys under aeroengine certification conditions. *Aerospace Lab*, 1–13 (2015). <https://doi.org/10.12762/2015.AL09-07>
- [12] Kromer, R., Mauget, F., Despres, L., Costil, S., Cormier, J.: Thermo-mechanical fatigue evaluation of a thermal barrier coating bond-coatless system. *Materials Science and Engineering: A* **756** (2019). <https://doi.org/10.1016/j.msea.2019.04.020>
- [13] Broomfield, R.W., Ford, D.A., Bhangu, J.K., Thomas, M.C., Frasier, D.J., Burkholder, P.S., Harris, K., Erickson, G.L., Wahl, J.B.: Development and Turbine Engine Performance of Three Advanced Rhenium Containing Superalloys for Single Crystal and Directionally Solidified Blades and Vanes. *Journal of Engineering for Gas Turbines and Power* **120**(3), 595–608 (1998). <https://doi.org/10.1115/1.2818188>
- [14] Leroy, M.: Étude de la nocivité d’un défaut de fonderie sur la durée de vie en fatigue à haute température d’une aube monocristalline, cas du joint de grains. PhD thesis, Mines Paristech (2013) <https://pastel.archives-ouvertes.fr/pastel-00963732/document>
- [15] Wang, R., Kanghe, F. J.and Jing, Hu, D.: Thermomechanical fatigue failure investigation on a single crystal nickel superalloy turbine blade. *Engineering Failure Analysis* **66**, 284–295 (2016). <https://doi.org/10.1016/j.engfailanal.2016.04.016>

- [16] Morar, N., Roy, R., J., M., Nicholls, J.R., Gray, S.: The effect of trepanning speed of laser drilled acute angled cooling holes on the high temperature low cycle corrosion fatigue performance of CMSX-4 at 850° C. *International Journal of Fatigue* **102**, 112–120 (2017). <https://doi.org/10.1016/j.ijfatigue.2017.04.017>
- [17] Zhou, Z.J., Wang, L., Wen, J.L., Lou, L.H., Zhang, J.: Effect of skew angle of holes on the tensile behavior of a ni-base single crystal superalloy. *Journal of Alloys and Compounds* **628** (2015). <https://doi.org/10.1016/j.jallcom.2014.12.096>
- [18] Pan, Y., Zimmer, R., Bischoff-Beiermann, B., Goldschmidt, D.: Fatigue behaviour of a single crystal nickel superalloy used in heavy-duty gas turbine blade with thin film cooling. In: *International Conference of Fracture*, Honolulu, USA (2001) <https://www.gruppofrattura.it/ocs/index.php/ICF/ICF10/paper/view/4660/6667>
- [19] Degeilh, R.: Experimental development and modelling of a thermal gradient mechanical fatigue test for single crystal turbine blade application (2013) [arg1](#)
- [20] Gallerneau, F., Kanoute, P., Roos, A.: Méthodologie de durée de vie dans les zones percées. Rapport technique RT1/13006 DMSM (2008). ONERA
- [21] Ryckelynck, D., Benziane, D.M.: Hyper-reduction framework for model calibration in plasticity-induced fatigue. *Advanced Modeling and Simulation in Engineering Sciences* **3**(15), 1–15 (2016). <https://doi.org/10.1186/s40323-016-0068-6>
- [22] Wahl, J.B., Harris, K.: CMSX-4 Plus Single Crystal Alloy Development, Characterization and Application Development. *Superalloys 2016*, 25–33 (2016). <https://doi.org/10.1002/9781119075646.ch3>
- [23] Huleux, V.: Comparaison des caractéristiques microstructurales et des propriétés en fluage de superalliages monocristallins à base de nickel de différentes générations. PhD thesis, Ecole des Mines de Paris - Université Paris Sciences et Lettres (2019). <https://doi.org/tel-02466605>
- [24] Versnyder, F.I., Shank, M.E.: The Development of Columnar Grain and Single Crystal High Temperature Materials through Directional Solidification. *Materials Science and Engineering*, vol. 6, 213–247 (1970) [https://doi.org/10.1016/0025-5416\(70\)90050-9](https://doi.org/10.1016/0025-5416(70)90050-9)
- [25] Reimers, P., Gilboy, W.B., Goebbels, J.: Recent developments in the industrial application of computerized tomography with ionizing radiation. *NDT International* **17**(4), 197–207 (1984). [https://doi.org/10.1016/0308-9126\(84\)90021-X](https://doi.org/10.1016/0308-9126(84)90021-X)

- [26] Ismail, I., Gamio, J.C., Bukhari, S.F.A., Yang, W.Q.: Tomography for multi-phase flow measurement in the oil industry. *Flow Measurement and Instrumentation* **16**(2), 145–155 (2005). <https://doi.org/10.1016/j.flowmeasinst.2005.02.017>. Tomographic Techniques for Multiphase Flow Measurements
- [27] Katunin, A., Dragan, K., Nowak, T., Chalimoniuk, M.: Quality control approach for the detection of internal lower density areas in composite disks in industrial conditions based on a combination of ndt techniques. *Sensors* **21**(21) (2021). <https://doi.org/10.3390/s21217174>
- [28] Gancarczyk, K., Albrecht, R., Bogdanowicz, W., Sieniawski, J.: Crystal Perfection Studies of Single Crystal Superalloy Turbine Blades by X-Ray Diffraction Methods. *Acta Physica Polonica A* **130**, 1088–1090 (2016). <https://doi.org/10.12693/APhysPolA.130.1088>
- [29] Arnaud, A., Guediche, W., Remacha, C., Romero, E., Proudhon, H.: A laboratory transmission diffraction Laue setup to evaluate single-crystal quality. *Journal of Applied Crystallography* **53** (2020). <https://doi.org/10.1107/S1600576720006317>
- [30] Frossard, L., Powrie, R., Langton, C.: In-vivo kinetic system to sustain residuum health of service members with lower limb loss: From proof-of-concept to digital twin. In: *Military Health System Research Symposium (MHSRS)*, pp. 1–1 (2019) <https://eprints.qut.edu.au/131940/>
- [31] Seon, G., Nikishkov, Y., Makeev, A., Ferguson, L.: Towards a digital twin for mitigating void formation during debulking of autoclave composite parts. *Engineering Fracture Mechanics* **225**, 106–792 (2020). <https://doi.org/10.1016/j.engfracmech.2019.106792>
- [32] Kianpour, E., Che Sidik, N., Golshokouh, I.: Film Cooling Effectiveness in a Gas Turbine Engine: A Review. *Jurnal Teknologi* **71**(2), 25–35 (2014). <https://doi.org/10.11113/jt.v71.3717>
- [33] Andersson, H.C.M., Sjöström, E.: Thermal gradients in round TMF specimens. *International Journal of Fatigue* **30**(2), 391–396 (2008). <https://doi.org/10.1016/j.ijfatigue.2007.01.050>. High Temperature Thermo-mechanical Fatigue: Testing Methodology, Interpretation of Data, and Applications
- [34] Esmaeilzadeh, M., Qods, F., Arabi, H., Sadeghi, B.M.: An investigation on crack growth rate of fatigue and induction heating thermo-mechanical fatigue (TMF) in Hastelloy X superalloy via LEFM, EPFM and integration models. *International Journal of Fatigue* **97**, 135–149 (2017). <https://doi.org/10.1016/j.ijfatigue.2016.12.036>

- [35] Beck, T., Hähner, P., Kühn, H.-J., Rae, C., Affeldt, E.E., Andersson, H., Köster, A., Marchionni, M.: Thermo-mechanical fatigue the route to standardisation (tmf-standard project). *Materials and Corrosion* **57**(1), 53–59 (2006). <https://doi.org/10.1002/maco.200503894>
- [36] Prasad, K., Kumar, V.: Isothermal and thermomechanical fatigue behaviour of ti6al4v titanium alloy. *Materials Science and Engineering: A* **528**(19), 6263–6270 (2011). <https://doi.org/10.1016/j.msea.2011.04.085>
- [37] Kupkovits, R.A., Neu, R.W.: Thermomechanical fatigue of a directionally-solidified Ni-base superalloy: Smooth and cylindrically-notched specimens. *International Journal of Fatigue* **32**(8), 1330–1342 (2010). <https://doi.org/10.1016/j.ijfatigue.2010.02.002>
- [38] Yang, J., Jing, F., Yang, Z., Jiang, K., Hu, D., Zhang, B.: Thermomechanical fatigue damage mechanism and life assessment of a single crystal Ni-based superalloy. *Journal of Alloys and Compounds* **872**, 159–578 (2021). <https://doi.org/10.1016/j.jallcom.2021.159578>
- [39] Kong, W., Wang, Y., Chen, Y., Liu, X., Yuan, C.: Investigation of uniaxial ratcheting fatigue behaviours and fracture mechanism of "GH742" superalloy at 923"K" **831**, 142–173 (2022). <https://doi.org/10.1016/j.msea.2021.142173>
- [40] Pei, H., Wang, J., Li, Z., Li, Z., Yao, X., Wen, Z., Yue, Z.: Oxidation behavior of recast layer of airfilm hole machined byEDM technology of Nibased single crystal blade and its effect on creep strength. *Surface and Coatings Technology* **419**, 127285 (2021). <https://doi.org/10.1016/j.surfcoat.2021.127285>
- [41] Kaminski, M.: Modélisation de l'endommagement en fatigue des superalliages monocristallins pour aubes de turbines en zone de concentration de contrainte. PhD thesis, École Nationale Supérieure des Mines de Paris (2007)
- [42] Sezer, H.K., Li, L., Schmidt, M., Pinkerton, A.J., Anderson, B., Williams, P.: Effect of beam angle on HAZ, recast and oxide layer characteristics in laser drilling of TBC nickel superalloys. *International Journal of Machine Tools and Manufacture* **46**(15), 1972–1982 (2006). <https://doi.org/10.1016/j.ijmachtools.2006.01.010>
- [43] Méric, L., Poubanne, P., Cailletaud, G.: Single Crystal Modeling for Structural Calculations: Part 1 Model Presentation. *Journal of Engineering Materials and Technology* **113**(1), 162–170 (1991). <https://doi.org/10.1115/1.2903374>